THE JOURNAL OF BIOLOGICAL CHEMISTRY VOL. 283, NO. 48, pp. 33087–33093, November 28, 2008
© 2008 by The American Society for Biochemistry and Molecular Biology, Inc. Printed in the U.S.A.

Antisense Masking Reveals Contributions of mRNA-rRNA Base Pairing to Translation of *Gtx* and *FGF2* mRNAs*[S]

Received for publication, June 27, 2008, and in revised form, October 1, 2008 Published, JBC Papers in Press, October 2, 2008, DOI 10.1074/jbc.M804904200

Panagiotis Panopoulos and Vincent P. Mauro[1]

From the Department of Neurobiology, The Scripps Research Institute and The Skaggs Institute for Chemical Biology, La Jolla, California 92037

We previously showed that a 9-nucleotide sequence from the 5′ leader of the *Gtx* homeodomain mRNA facilitates translation initiation by base pairing to 18S rRNA. These earlier studies tested the *Gtx* element in isolation; we now assess the physiological relevance of this element in the context of two natural mRNAs that contain this sequence in their 5′ leaders, *Gtx* itself and *FGF2* (fibroblast growth factor 2). 2′-*O*-Methyl-modified RNA oligonucleotides were employed to block mRNA-rRNA base pairing by targeting either the *Gtx*-binding site in 18S rRNA or *Gtx* elements in recombinant mRNAs containing the *Gtx* or *FGF2* 5′ leaders linked to a reporter cistron. Studies in cell-free lysates and transfected COS-7 cells showed that translation of mRNAs containing the *Gtx* or *FGF2* 5′ leaders was decreased by >50% when oligonucleotides targeting either the rRNA or mRNA were used. Specificity was demonstrated by showing that translation of the recombinant mRNAs was unaffected by control oligonucleotides. In addition, the specific oligonucleotides did not affect the translation of recombinant mRNAs in which the *Gtx* elements were mutated. Experiments performed using constructs containing *Gtx* and *FGF2* 5′ leader and coding sequences ruled out possible effects of the reporter cistron. Furthermore, two-dimensional gel electrophoresis revealed that the oligonucleotides used in this study had little overall effect on the proteomes of cells transfected with these oligonucleotides. This study demonstrates that mRNA-rRNA base pairing affects the expression of two cellular mRNAs and describes a new approach for investigating putative mRNA-rRNA base pairing interactions in mammalian cells.

Numerous mRNAs contain complementary matches to 18S rRNA, and it has been suggested that such sequences may affect translation by base pairing to each other (1–3). In earlier studies, we noted that the 5′ leader of the *Gtx* homeodomain mRNA contains a 9-nucleotide sequence with complementarity to sequences contained within helix 26 of mouse 18S rRNA (4). Biochemical, functional, and genetic studies showed that this sequence element could mediate specific binding to 40S ribosomal subunits by base pairing to 18S rRNA and function as an internal ribosome entry site and as a translational enhancer element (TEE)[2] and ribosomal shunt site (3, 5–8). We showed that this element could function in isolation and as a modular component of larger assemblages of elements, with additive or synergistic enhancements of activity depending on the nucleotide context and message configuration (3). These properties of the *Gtx* element facilitated our analysis of its mechanism because the ability of the individual element to affect translation is relatively weak. However, the relatively weak activity of a single *Gtx* element raised questions regarding its physiological relevance. It was therefore important to perform studies to determine whether an individual *Gtx* element affects translation efficiency in the context of natural mRNAs that contain this sequence. In this study, we investigate the physiological contribution of the *Gtx* element to the translation of two such mRNAs: *Gtx* and *FGF2* (fibroblast growth factor 2).

The murine *Gtx* mRNA, also termed *Nkx 6-2*, is expressed in differentiated oligodendrocytes and testis germ cells (9, 10). The 5′ leader is 201 nucleotides in length, and the TEE is located 56 nucleotides upstream of the initiation codon. This mRNA encodes a homeobox protein that binds to DNA sequences within the promoters of the myelin basic protein and proteolipid protein genes (9) and is thought to have a role in regulating myelin gene transcription in oligodendrocytes. The 5′ leader of the human *FGF*2 mRNA also contains a sequence matching the *Gtx*-TEE (11, 12). Inasmuch as the sequence of the *Gtx*-binding site in rodent 18S rRNA is also found in humans, we chose the *FGF2* mRNA for further analysis. The 5′ leader of this mRNA is 471 nucleotides in length and expresses five FGF2 isoforms from different initiation codons, including four noncanonical CUG codons and an AUG codon (13–15). The *Gtx* element is located at nucleotides 119–127, upstream of three CUG codons and the AUG codon. It is downstream of the first CUG codon, which is cap-dependent (16). In this mRNA, the complementary match to 18S rRNA (13 of 14 nucleotides) is even more extensive than in the *Gtx* mRNA. The various FGF2 isoforms differ in subcellular localization, function, and relative abundance in different cells and tissues (15, 17–23) and are involved in fundamental cellular processes, which include cell proliferation, differentiation, and angiogenesis (23).

* This work was supported, in whole or in part, by National Institutes of Health Grant GM078071 (to V. P. M.). This work was also supported by the Skaggs Institute for Chemical Biology (to P. P.). The costs of publication of this article were defrayed in part by the payment of page charges. This article must therefore be hereby marked "*advertisement*" in accordance with 18 U.S.C. Section 1734 solely to indicate this fact.

[S] The on-line version of this article (available at http://www.jbc.org) contains supplemental Figs. 1 and 2.

[1] To whom correspondence should be addressed: 10550 North Torrey Pines Rd., La Jolla, CA 92037. Tel.: 858-784-2600; Fax: 858-784-2646; E-mail: vmauro@scripps.edu.

[2] The abbreviations used are: TEE, translational enhancer element; nt, nucleotide; LC/MS/MS, liquid chromatography/tandem mass spectrometry; BisTris, 2-[bis(2-hydroxyethyl)amino]-2-(hydroxymethyl)propane-1,3-diol; CHAPS, 3-[(3-cholamidopropyl)dimethylammonio]-1-propanesulfonic acid.

This study investigates the extent to which the *Gtx* element contributes to the translation of the *Gtx* and *FGF2* mRNAs by using antisense oligonucleotides to block either the *Gtx*-binding site in 18S rRNA or the *Gtx* element in either the *Gtx* or the *FGF2* mRNAs. We expect that this antisense masking approach can also be used to identify other natural mRNAs that employ mRNA-rRNA base pairing, either via the *Gtx* element or through other binding sites in the 18S rRNA.

EXPERIMENTAL PROCEDURES

DNA Constructs—Monocistronic constructs included those containing the *Gtx* and *FGF2* 5′ leaders linked to the *Photinus* luciferase cistron, as well as those containing these 5′ leaders linked to the corresponding *Gtx* or *FGF2* coding sequences. Luciferase reporter constructs were generated using the pGL3c (Promega) plasmid, which expresses the mRNA via the SV40 promoter. The *Gtx* and *FGF2* 5′ leader sequences were synthesized by PCR amplification of oligonucleotide templates and cloned upstream of the *Photinus luciferase* cistron. Briefly, constructs expressing the *Gtx* 5′ leader and either the *Gtx* or luciferase coding sequences were cloned using AatII and NcoI restriction sites. The AatII site was introduced at the transcription start site to avoid inclusion of vector-derived sequence in the recombinant transcripts; the NcoI site contains the initiation codon. The *Gtx* coding sequences were obtained by PCR amplification of mouse genomic DNA. The PCR-generated fragment was digested with NcoI and XbaI, which was introduced through the PCR primer, and cloned into the vector containing the *Gtx* 5′ leader, as described above. Constructs containing the *FGF2* 5′ leader and luciferase or *FGF2* coding sequences were similarly constructed except that the *FGF2* coding sequences were synthesized by PCR amplification of oligonucleotide templates. Mutations in the *Gtx* element were introduced into the *Gtx* 5′ leader using annealed oligonucleotides that generated a 43-nt fragment with ApaI/BssHII sticky ends. For FGF2, annealed oligonucleotides generated a 38-nt fragment with SacII sticky ends. In both cases, the annealed oligonucleotides were used to replace the corresponding fragments from the 5′ leader.

Oligonucleotides—2′-*O*-Methyl-modified RNA oligonucleotides were obtained from Thermo Scientific (Dharmacon RNAi Technologies). Oligonucleotide sequences are as follows, with the noncomplementary nucleotides in the *Gtx*-m1 and *α-Gtx*-m1 oligonucleotides underlined: *Gtx*, 5′ CCGGCGGGU 3′; *Gtx*-m1, 5′ CCGG<u>A</u>GGGU 3′; *α-Gtx*, 5′ ACCCGCCGG 3′; *α-Gtx*-m1, 5′ ACCC<u>A</u>CCGG 3′; and *Gtx*-scrambled, 5′ CGGCGCUGG 3′.

In Vitro Translation—Capped mRNAs were generated from plasmids linearized using ClaI, which is located downstream of the luciferase cistron, and were transcribed by using the mMessage mMachine (Ambion). RNAs were quantified by UV absorption at 260 nm. *In vitro* translation reactions were performed in rabbit reticulocyte lysate as specified by the manufacturer (Promega) with the following modification: translation reactions were performed in 10 μl and incubated for 15 min at 37 °C instead of the proposed 50 μl reactions incubated at 37 °C for 90 min. These conditions were determined to be in the linear phase of the translation reaction.

Transfection—FuGENE 6 (Roche Diagnostics) was used to transfect 1–3 × 10^5 COS-7 cells with 0.5 μg of reporter construct according to the manufacturer's instructions. Cells were cotransfected either with a control construct p(SI/SIII)$_5$βP (6), which expresses *Photinus* luciferase, or pCMVβ (Clontech), which expresses the *lacZ* gene. Neither of the control mRNAs contain sequences similar to the *Gtx* element. Transfected cells were harvested 18–24 h after transfection, and luciferase and β-galactosidase activities were determined as described previously (6). 2′-*O*-Methyl-modified RNA oligonucleotides were cotransfected with plasmids or were transfected alone using the abovementioned conditions at concentrations indicated in the figures.

Analyses of Reporter Gene Activity and mRNA Levels—Luciferase activities were determined as described previously (6). Recombinant mRNA levels were determined by using ribonuclease protection assays (RPAIII kit; Ambion) with 1 μg of DNase-treated total RNA. Protected fragments were size-fractionated on 6% polyacrylamide-urea gels, visualized on a Storm 860 PhosphorImager (GE Healthcare), and quantified by using ALPHAEASEFC stand-alone software (Alpha Innotech, San Leandro, CA).

Western Immunoblotting—Cell lysates were prepared 18–24 h after transfection; cell monolayers were scraped, resuspended in lysis buffer (RIPA Buffer: 50 mM Tris-HCl, pH 7.4, 150 mM NaCl, 1 mM EDTA, 1% Triton X-100, 0.1% SDS, 1% sodium deoxycholate, and 1× complete mix of protease inhibitor), and sonicated. Total protein in cell lysates was quantified using the Bio-Rad DC protein assay kit. For Western blots, samples containing 25 μg of protein were heated for 10 min at 72 °C in SDS and dithiothreitol-containing sample buffer and separated in a 4–12% gradient BisTris polyacrylamide gel (Invitrogen). Proteins were transferred to polyvinylidene difluoride membranes and probed with goat anti-*Gtx* or anti-*FGF2* polyclonal IgG 1° antibodies (Santa Cruz Biotechnology) and visualized using the CDP Star chemiluminescent Western blot immunodetection kit (Roche Applied Science) with donkey anti-goat IgG 2° antibody conjugated to alkaline phosphatase (Promega). For control experiments, an anti-β-actin monoclonal mouse IgG 1° antibody (Sigma) and an anti-mouse IgG 2° antibody (Sigma) conjugated to alkaline phosphatase were used to detect the β-actin protein.

Two-dimensional Gel Electrophoresis—Cell lysates were prepared 18–24 h after transfection by scraping the cell monolayers, resuspending in lysis buffer (50 mM Tris-HCl, pH 7.4, 20 mM NaCl, and 1% IGEPAL detergent), and sonicating. Total protein in cell lysates was quantified as above. Protein samples (50 μg per gel) were diluted to 125 μl in rehydration buffer (8 M urea, 2% CHAPS, 50 mM dithiothreitol, 0.2% Bio-Lyte ampholytes, and 0.002% bromphenol blue). The indicated volume of each sample was applied to a gel strip (17 cm, pH 3–10, Bio-Rad), rehydrated for 16–20 h, and focused using a PROTEAN isoelectric focusing cell and in three steps as follows: 1) 250 V, 1 h linear; 2) 1000 V, 2 h linear; and 3) 10,000 V, 45,000 V-h rapid. Prior to running the second dimension, gel strips were either stored at −70 °C or equilibrated in 2 ml of equilibration buffer 1 (6 M urea, 0.375 M Tris-HCl, pH 8.8, 2% SDS, 20% glycerol, 2% w/v dithiothreitol) for 10 min. Isoelectric focusing strips were then equilibrated in equilibration buffer 2

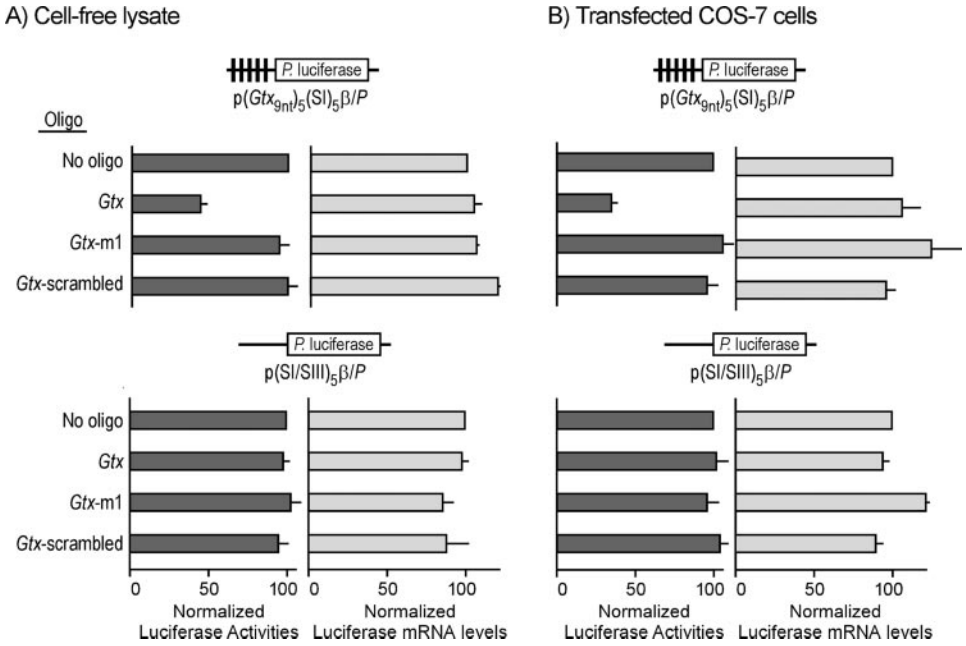

FIGURE 1. **Oligonucleotide masking of *Gtx*-binding site in 18S rRNA blocks activity of isolated *Gtx* elements in rabbit reticulocyte cell-free lysate (*A*) and transiently transfected COS-7 cells (*B*).** The constructs used in this study are indicated schematically. *Vertical black bars* in the 5′ leader of the p(Gtx_{9nt})$_5$(SI)$_5\beta/P$ mRNA represent 9-nt *Gtx* elements. Control construct p(SI/SIII)$_5\beta/P$ is a size-matched control that lacks *Gtx* elements. The absence or presence of specific oligonucleotides (*oligo*) is indicated. *A* and *B*, oligonucleotide concentration is 1 μM, and luciferase activities or luciferase mRNA levels for each construct are normalized to 100 for the activity of the no oligonucleotide control. The data points represent the results of three independent experiments; the *error bars* indicate S.E.

(6 M urea, 0.375 M Tris-HCl, pH 8.8, 2% SDS, 20% glycerol, 2.5% w/v iodoacetamide) for 10 min and run on 12% acrylamide SDS-polyacrylamide gels.

Protein spots were stained using the Flamingo fluorescent gel stain (Bio-Rad), visualized at 532 nm using the Typhoon Trio Variable Mode Imager (GE Healthcare), and analyzed using the Progenesis SameSpots computer software (Nonlinear Dynamics, Durham, NC). Protein spots were reduced in-gel using 10 mM dithiothreitol, alkylated with 55 mM iodoacetamide, and digested with trypsin in an estimated 1:30 enzyme to substrate ratio. The samples were then analyzed using the Agilent MSD 1100 nano-electrospray LC/MS/MS. MS/MS analysis was performed on the LTQ linear ion trap mass spectrometer (Thermo) using 2 kV at the tip. One MS spectrum was followed by four MS/MS scans on the most abundant ions after the application of the dynamic exclusion list. Tandem mass spectra were subjected to peak picking using Xcalibur (version 2.0 SR2, Thermo Electron Corp.). Protein identification was performed using Mascot (version 2.1.04, Matrix Science, London, UK).

Proteins were identified using a Mascot search (version 2.1.04, Matrix Science, London, UK) at a 95% confidence level using a data base of tryptic peptides derived from the NCBI annotation of primate genomes (June 6, 2008). Scores were adjusted to give a false-positive rate of <1% based on a decoy data base search. An ion score threshold of 35 gave an acceptable and low false-positive rate of 0.398 ± 0.57% using a dataset of 20 searches. All searches were done using this threshold, which included single peptide assignments that were included in the analysis.

RESULTS

Oligonucleotide Masking of Gtx-binding Site in 18S rRNA Blocks Activity of Isolated Gtx Elements—The feasibility of using oligonucleotides to block the base pairing interaction between the *Gtx* TEE and 18S rRNA was tested using synthetic mRNA constructs containing five linked copies of the *Gtx* TEE in the 5′ leader of the *Photinus* luciferase mRNA. Comparable constructs were used in our earlier work to study this element in isolation (3, 6–8). Constructs were tested both in rabbit reticulocyte lysate using mRNAs transcribed with T7 RNA polymerase and in transfected cells, with transcription driven by the SV40 promoter.

For these studies, we used 2′-*O*-methyl-RNA oligonucleotides, which contain a methyl group at the 2′-OH residue of the ribose molecule. These modified oligonucleotides base pair with RNA more stably than DNA or unmodified RNA oligonucleotides; they are also more resistant to nuclease degradation than unmodified RNA oligonucleotides and do not target the hybridized region of the target RNA to digestion by RNase H, which is a potential limitation associated with DNA oligonucleotides (24–26).

The results showed that increasing concentrations of the *Gtx* oligonucleotide, which targets the *Gtx*-binding site in 18S rRNA (nucleotides 1124–1132), led to progressively reduced luciferase activities from a construct containing five *Gtx* TEEs (p(Gtx_{9nt})$_5$(SI)$_5\beta/P$) either in an *in vitro* translation assay or in COS-7 transfected cells (supplemental Fig. 1*A*). Construct p*Gtx*/*P* containing the full-length *Gtx* 5′ leader exhibited a similar trend both *in vitro* and in transfected COS-7 cells (supplemental Fig. 1*B*). Maximal inhibition was obtained using 1 μM both in the cell-free lysate and in cells. Cell-free studies were performed using *in vitro* transcribed *Gtx* reporter mRNAs in the absence or presence of the *Gtx*, scrambled, and *Gtx*-m1 oligonucleotides. Fig. 1*A* shows results obtained in the cell-free lysate with the reporter construct containing five *Gtx* TEEs (p(Gtx_{9nt})$_5$(SI)$_5\beta/P$) and 1 μM of the *Gtx* oligonucleotide. Luciferase expression was reduced by ≈50% compared with samples containing the *Gtx* reporter construct alone (no oligonucleotide). Control experiments using a scrambled oligonucleotide (*Gtx*-scrambled) and an oligonucleotide with a point mutation in the *Gtx* sequence (*Gtx*-m1) had no effect on luciferase expression, suggesting that the *Gtx* oligonucleotide specifically blocked the activity of the *Gtx* elements. Expression of a control construct (p(SI/SIII)$_5\beta/P$) lacking *Gtx* elements was unaffected by any of the oligonucleotides, suggesting that the *Gtx* oligonu-

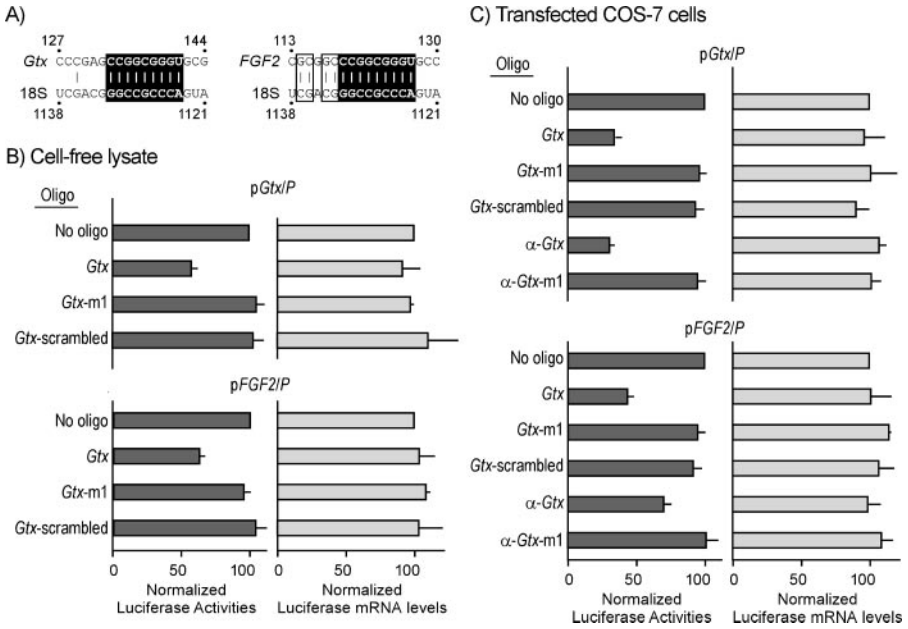

FIGURE 2. **Oligonucleotide masking of rRNA or mRNA sequences blocks translation of luciferase reporter mRNAs containing full-length *Gtx* and *FGF2* 5′ leaders.** *A,* complementary matches between nucleotides in mouse 18S rRNA and *Gtx* 5′ leader or human 18S rRNA and *FGF2* 5′ leader. *B,* expression in rabbit reticulocyte lysate. *C,* transiently transfected COS-7 cells. Constructs p*Gtx/P* and p*FGF2/P* contain the *Gtx* and *FGF2* 5′ leaders, respectively, upstream of the *Photinus* luciferase cistron. The absence or presence of oligonucleotides (*oligo*) (1 μM) is indicated. For each construct, luciferase activities or luciferase mRNA levels for each construct are normalized to 100 for the activity of the no oligonucleotide control. The data points represent the results of three independent experiments; the *error bars* indicate S.E.

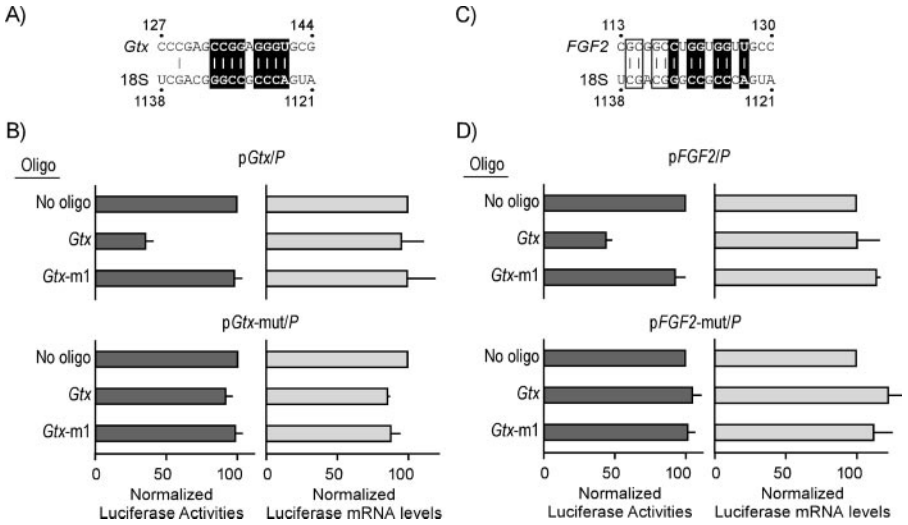

FIGURE 3. **Mutation of *Gtx* TEE in *Gtx* or *FGF2* 5′ leaders prevents inhibition by antisense masking.** Constructs p*Gtx/P* and p*FGF2/P* contain the *Gtx* or *FGF2* 5′ leaders, respectively, linked to *Photinus* luciferase. Constructs p*Gtx*-mut/*P* and p*FGF2*-mut/*P* are identical except for point mutations in the *Gtx* elements, which are shown in *A* for the *Gtx* 5′ leader and in *B* for the *FGF2* 5′ leader. Constructs were expressed in transiently transfected COS-7 cells. The results obtained with the *Gtx* constructs are shown in *C* and those with the *FGF2* 5′ leader in *D*. The absence or presence of oligonucleotides (*oligo*) (1 μM) is indicated. Luciferase activities or luciferase mRNA levels for each construct are normalized to 100 for the no oligonucleotide control. The data points represent the results of three independent experiments; the *error bars* indicate S.E.

cleotide affected translation of the *Gtx* reporter mRNA by blocking the activity of *Gtx* TEEs. These results are consistent with direct inhibition by the *Gtx* oligonucleotide of mRNA-rRNA base pairing. RNA analyses indicated that the decreased luciferase levels observed in samples incubated with the *Gtx* oligonucleotide were not because of decreased reporter mRNA levels but to a decrease in translation efficiency.

Fig. 1*B* shows that comparable results were obtained when COS-7 cells were cotransfected with the reporter construct containing five *Gtx* TEEs and 1 μM of the *Gtx* oligonucleotide. Luciferase expression was reduced by ≈60% compared with cells transfected with the reporter construct alone (no oligonucleotide). The control oligonucleotides did not affect luciferase expression. In addition, control construct p(SI/SIII)$_5\beta/P$ was unaffected by any of the oligonucleotides. RNA analysis indicated that decreased luciferase levels in cells cotransfected with the *Gtx* oligonucleotide were not because of decreased reporter mRNA levels but to a decrease in translation efficiency.

Antisense Masking Establishes Contribution of Gtx Elements in Gtx and FGF2 5′ Leaders—To begin to assess the contribution of an individual *Gtx* element in the context of a natural mRNA, we investigated the *Gtx* 5′ leader, which was the source of this element. In addition, we investigated the *FGF2* 5′ leader, which contains the nucleotide sequence of the *Gtx* element as well as a more extended complementary match to 18S rRNA (Fig. 2*A*). The contributions of these individual *Gtx* elements were initially tested using *Photinus* luciferase reporter constructs as follows: p*Gtx*/*P* and *FGF2*/*P*, containing the full-length *Gtx* 5′ leader (201 nt), or *FGF2* 5′ leader (471 nt). The contribution of the *Gtx* element to the translation mediated by these two 5′ leaders was assessed using the *Gtx* oligonucleotide to block the *Gtx*-binding site in 18S rRNA in both a rabbit reticulocyte cell-free lysate and transfected COS-7 cells. The results showed that this oligonucleotide blocked expression mediated by the *Gtx* 5′ leader by ≈45% in the cell-free lysate (Fig. 2*B*) and ≈65% in transfected cells (Fig. 2*C*). In contrast, expression remained unaffected in both the cell-free lysate and transfected cells upon exposure to the mutated *Gtx*-m1 oligonucleotide. In addition, in both systems, expression from a control RNA lacking *Gtx* elements was unaffected by the *Gtx* oligonucleotide. The control *Gtx*-m1 and *Gtx*-scrambled oligonucleotides had no effect on the expression of

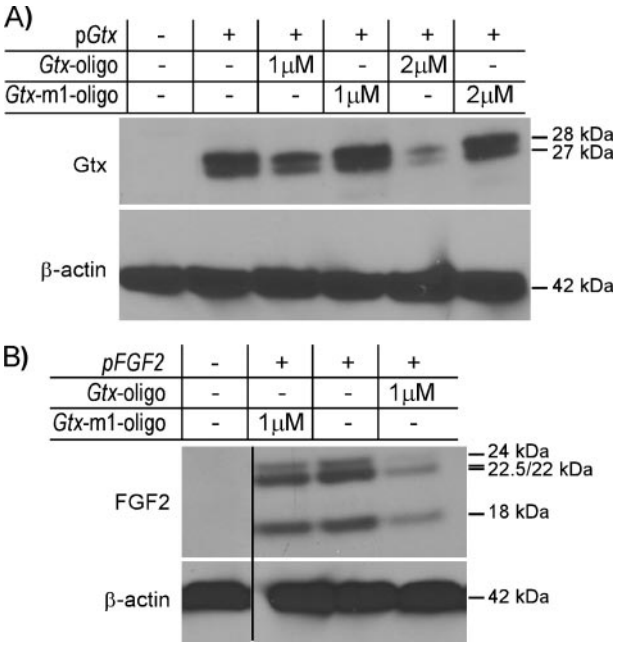

FIGURE 4. **Oligonucleotide masking of *Gtx*-binding site in 18S rRNA blocks activity of recombinant mRNAs.** Plasmids containing *Gtx* (p*Gtx*) (*A*) or *FGF2* (p*FGF2*) (*B*) 5′ leader and coding sequences were transiently transfected into COS-7 cells and cell lysates analyzed by Western blot analysis using anti-Gtx, anti-FGF2, or anti-β-actin antibodies as indicated. *Histogram* above Western blots indicates plasmids and oligonucleotides (*oligo*) in the various samples. Molecular weights of Gtx, FGF2, and β-actin protein bands are indicated to the *right*. This experiment was repeated with similar results three times.

any of these constructs. Experiments performed using constructs containing full-length *FGF2* 5′ leader yielded similar results, with the *Gtx* oligonucleotide blocking expression by ≈40% in the cell-free lysate (Fig. 2*B*) and 55% in the transfected cells (Fig. 2*C*). Furthermore, expression of both p*Gtx*/*P* and *FGF2*/*P* constructs was blocked by approximately the same amount by an oligonucleotide targeting the *Gtx* element in the mRNA (α-*Gtx*). In contrast, expression was unaffected by a mutated α-*Gtx* oligonucleotide (α-*Gtx*-m1; Fig. 2*C*). The control construct was unaffected by any of the oligonucleotides in both systems (data not shown). Ribonuclease protection assays showed that the reporter mRNA levels were unaffected in cells transfected with the various oligonucleotides, suggesting that the effects observed were not due to altered mRNA levels (Fig. 2, *B* and *C*).

To further evaluate the specificity of the results, *Gtx* elements in the two 5′ leaders were disrupted by point mutations within the *Gtx* element (Fig. 3, *A* and *C*). The point mutation in the *Gtx* 5′ leader (in p*Gtx*-mut/*P*) was known from earlier studies to block the activity of the *Gtx*-TEE (8). In these studies, this mutation reduced luciferase expression by ≈40% in transfected cells. For the *FGF2* 5′ leader, we introduced three point mutations to disrupt possible base pairing interactions to 18S rRNA because this 5′ leader contains a more extensive complementary match. These point mutations in the *FGF2* 5′ leader (in p*FGF2*-mut/*P*) reduced expression by 25%. The *Gtx* oligonucleotide did not affect expression from the mutated *Gtx* construct, similar to the controls (No oligonucleotide and *Gtx*-m1; Fig. 3*B*). Likewise, the *Gtx* oligonucleotide did not affect expression from the mutated *FGF2* construct (Fig. 3*D*). Ribonuclease protection assays showed that the reporter mRNA levels were relatively unaffected in cells transfected with the various oligonucleotides, suggesting that the effects observed were not due to altered mRNA levels (Fig. 3, *B* and *D*).

Evaluating Effects of Coding Sequences—To rule out possible nonspecific effects of the luciferase reporter cistron, we tested constructs containing both the *Gtx* and *FGF2* 5′ leader and coding sequences in COS-7 cells and evaluated expression by immunoblot analyses using anti-Gtx and anti-FGF2 antibodies, respectively. The results showed that each of these mRNAs produced several protein bands (Fig. 4, *A* and *B*). The two Gtx bands correspond to the full-length protein and a shorter product initiating from an in-frame AUG codon in the coding region. The FGF2 bands correspond to initiation from the initiation codon and three upstream CUG codons. In cells cotransfected with 1 μM of the *Gtx* oligonucleotide, levels of the Gtx and FGF2 proteins decreased. For Gtx, this decrease was even greater in the presence of 2 μM oligonucleotide. In contrast, the levels of these proteins were similar to those in control cells when cells were exposed to the mutated (*Gtx*-m1) oligonucleotide. Immunoblot analyses using an anti-β-actin antibody showed that the levels of endogenous β-actin were unaffected by the *Gtx* oligonucleotide, further suggesting that the effects of this oligonucleotide were specific.

Assessing the Effects of Gtx and α-Gtx Oligonucleotides on the Proteome—The specificity of the *Gtx* and α-*Gtx* oligonucleotides was further evaluated by looking at their effects on the proteome. These effects were monitored by two-dimensional gel electrophoresis. COS-7 cells were transiently transfected with the *Gtx* oligonucleotide. Cells were lysed, and proteins in these lysates were compared with those from untransfected COS-7 cells using two-dimensional gel electrophoresis (Fig. 5). Comparison of the gels showed that the overall pattern of proteins, as well as the relative levels of proteins, was highly similar. The SameSpots computer software was used to match and quantify protein spots between gels. When the gel containing proteins from untransfected COS-7 cells (Fig. 5*A*) was compared with the gel with protein from COS-7 cells transfected with the *Gtx* oligonucleotide (Fig. 5*B*), 12 of 196 spots showed a significant change in expression. In addition, when two-dimensional gels containing proteins from untransfected COS-7 cells were compared with those from cells transiently transfected with the *Gtx*-m1 and α-*Gtx* oligonucleotides (not shown), we found that five of these spots changed only with the *Gtx* and α-*Gtx* oligonucleotides, suggesting that the expression of these five proteins may involve base pairing interactions mediated by *Gtx* elements. The intensity (volume) of these spots was inhibited by 30–55% compared with the same spots from untransfected cells. These spots were picked from the two-dimensional gels, digested, and analyzed using a nano-LC/MS/MS method. We were able to identify proteins from two spots with >95% confidence as follows: vimentin (gi/75075845), an intermediate filament protein, and stomatin (gi/7305503), a component of lipid rafts. The 5′ leaders of the mRNAs encoding these proteins were analyzed for the presence of a *Gtx* element or elements. This analysis revealed that both the 186-nt *vimentin* 5′ leader and the 63-nt *stomatin* 5′ leader contain 7- and 6-nt

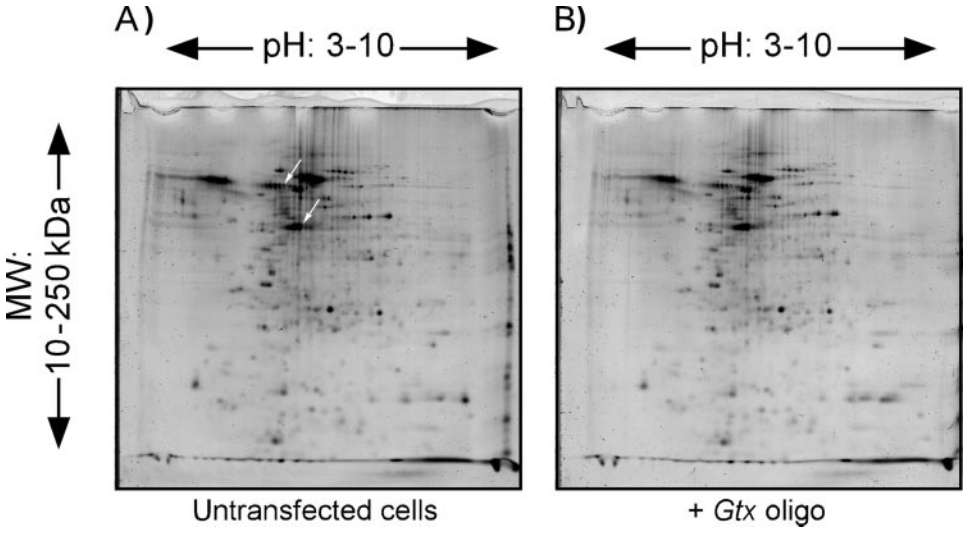

FIGURE 5. **Two-dimensional gel electrophoresis of COS-7 proteins in the absence or presence of masking or control oligonucleotides.** Proteins were electrophoresed from COS-7 cells that were either untransfected (*A*) or transfected (*B*) with 1 μM *Gtx* oligonucleotide (*oligo*). The *arrows* in *A* are spots that were subjected to mass spectrometry and correspond to vimentin (*upper arrow*) and stomatin (*lower arrow*).

contiguous matches to the *Gtx* element, respectively (supplemental Fig. 2). Our earlier studies showed that comparable matches were functional and could be as active or more active than the 9-nt element (6, 8).

DISCUSSION

Base pairing between mRNA and rRNA underlies the well established Shine-Dalgarno interaction in bacteria (27, 28). Our earlier analysis of the *Gtx* TEE indicated that similar base pairing interactions were not limited to bacteria but could also occur in eukaryotes (6, 8). These earlier studies required testing the *Gtx* TEE as an isolated element, *i.e.* outside of the *Gtx* 5′ leader from which it was identified. This study now provides the first evidence that mRNA-rRNA base pairing can affect the translation of some mammalian mRNAs.

In this study, we showed that oligonucleotides targeting either the *Gtx*-binding site in 18S rRNA or the *Gtx* TEE in the *Gtx* and *FGF2* 5′ leaders reduced translation from mRNAs containing these 5′ leaders. In addition, mRNAs in which the *Gtx* TEEs were mutated were translated less efficiently, suggesting that the *Gtx* TEE enhances translation in the *Gtx* and *FGF2* mRNAs. Moreover, the mutated mRNAs were no longer affected by the *Gtx* oligonucleotide, indicating that the inhibitory effect of this oligonucleotide involved blocking the activity of the TEE.

Antisense masking of the binding site in 18S rRNA enabled us to assess the contribution of the *Gtx* TEE in mRNAs without mutating, deleting, or otherwise modifying the mRNAs. This is an important advantage of the approach because any of these manipulations may themselves have nonspecific effects on expression, *e.g.* by affecting RNA conformation or altering the accessibility of other mRNA elements, including initiation codons (7). Such effects may underlie the results of a study in which deletion of a segment of the *FGF2* 5′ leader containing the *Gtx* TEE led to significantly decreased translation (11), which is consistent with our findings, but various other mutations of the *Gtx* TEE or flanking nucleotides yielded inconsistent results.

A limitation of the antisense masking approach is that it cannot distinguish between an mRNA element that binds to 18S rRNA or to another RNA. This is not a serious concern for the *Gtx* TEE because there is both biochemical as well as genetic evidence indicating that this element binds specifically to helix 26 of 18S rRNA and not to other factors (4, 6, 8). However, for a different mRNA element, additional evidence would be required to establish that the element is base pairing to rRNA. Ideally, one would perform experiments involving mutation of both mRNA and rRNA sequences to assess the requirement for an intact complementary match. Such a genetic approach was used to confirm the Shine-Dalgarno interaction in *Escherichia coli* (28). We used a similar approach in yeast to establish the *Gtx* interaction (8). Although a suitable system for performing comparable studies in mammalian cells does not yet exist, we have undertaken studies in our laboratory to develop such a system.

The oligonucleotides used in our studies did not appear to have global effects on the proteomes of cells transfected with them, as monitored by two-dimensional gel electrophoresis. However, the levels of a small number of proteins did change specifically with the *Gtx* and α-*Gtx* oligonucleotides, suggesting that the translation of mRNAs encoding these proteins is affected by base pairing to the *Gtx*-binding site in 18S rRNA. Indeed, mass spectrometry of two proteins showing such a change revealed that the corresponding mRNAs contain matches to the *Gtx* element in their 5′ leaders, which provides a plausible explanation for the effects of *Gtx* and α-*Gtx* oligonucleotides. The changes observed in the levels of proteins affected by both the *Gtx* and α-*Gtx* oligonucleotides in COS-7 cells is consistent with the total number of mRNAs containing sequences complementary to the *Gtx*-binding site in 18S rRNA ($<$1%).

The observation that numerous eukaryotic mRNAs contain sequences with complementarity to different sites in the 18S rRNA (*e.g.* see Refs. 1, 2, 29, 30) raises the possibility that the translation of a reasonably large number of eukaryotic mRNAs may be affected by base pairing to ribosomes. In contrast to the Shine-Dalgarno sequence in prokaryotes, which is located upstream of and in close proximity to the initiation codon, sequences with complementarity to rRNA in eukaryotic mRNAs are not restricted to the region located immediately upstream of the initiation codon but are found in all parts of mRNAs. Likewise, putative binding sites in 18S rRNA are not restricted to the 3′ end but are found throughout the molecule.

This study provides the first evidence indicating that the translation efficiency of some natural mRNAs is affected by

base pairing to the *Gtx*-binding site in 18S rRNA. In addition, this study provides an experimental approach for investigating putative mRNA-rRNA base pairing interactions in mammalian cells via the *Gtx*-binding site in 18S rRNA as well as through other possible binding sites.

Acknowledgments—We thank Luke Burman for excellent technical assistance and Dr. Gerald M. Edelman for critical reading of the manuscript.

REFERENCES

1. Scheper, G. C., Voorma, H. O., and Thomas, A. A. M. (1994) *FEBS Lett.* **352,** 271–275
2. Mauro, V. P., and Edelman, G. M. (1997) *Proc. Natl. Acad. Sci. U. S. A.* **94,** 422–427
3. Chappell, S. A., Edelman, G. M., and Mauro, V. P. (2000) *Proc. Natl. Acad. Sci. U. S. A.* **97,** 1536–1541
4. Hu, M. C.-Y., Tranque, P., Edelman, G. M., and Mauro, V. P. (1999) *Proc. Natl. Acad. Sci. U. S. A.* **96,** 1339–1344
5. Chappell, S. A., Dresios, J., Edelman, G. M., and Mauro, V. P. (2006) *Proc. Natl. Acad. Sci. U. S. A.* **103,** 9488–9493
6. Chappell, S. A., Edelman, G. M., and Mauro, V. P. (2004) *Proc. Natl. Acad. Sci. U. S. A.* **101,** 9590–9594
7. Chappell, S. A., Edelman, G. M., and Mauro, V. P. (2006) *Proc. Natl. Acad. Sci. U. S. A.* **103,** 18077–18082
8. Dresios, J., Chappell, S. A., Zhou, W., and Mauro, V. P. (2006) *Nat. Struct. Mol. Biol.* **13,** 30–34
9. Awatramani, R., Scherer, S., Grinspan, J., Collarini, E., Skoff, R., O'Hagan, D., Garbern, J., and Kamholz, J. (1997) *J. Neurosci.* **17,** 6657–6668
10. Ren, B., Robert, F., Wyrick, J. J., Aparicio, O., Jennings, E. G., Simon, I., Zeitlinger, J., Schreiber, J., Hannett, N., Kanin, E., Volkert, T. L., Wilson, C. J., Bell, S. P., and Young, R. A. (2000) *Science* **290,** 2306–2309
11. Bonnal, S., Schaeffer, C., Creancier, L., Clamens, S., Moine, H., Prats, A. C., and Vagner, S. (2003) *J. Biol. Chem.* **278,** 39330–39336
12. Vagner, S., Gensac, M. C., Maret, A., Almaric, F., Prats, H., and Prats, A. C. (1995) *Mol. Cell. Biol.* **15,** 35–44
13. Florkiewicz, R. Z., and Sommer, A. (1989) *Proc. Natl. Acad. Sci. U. S. A.* **86,** 3978–3981
14. Prats, H., Kaghad, M., Prats, A. C., Klagsbrun, M., Lelias, J. M., Liauzun, P., Chalon, P., Tauber, J. P., Amalric, F., Smith, J. A., and Caput, D. (1989) *Proc. Natl. Acad. Sci. U. S. A.* **86,** 1836–1840
15. Arnaud, E., Touriol, C., Boutonnet, C., Gensac, M. C., Vagner, S., Prats, H., and Prats, A. C. (1999) *Mol. Cell. Biol.* **19,** 505–514
16. Yu, P. J., Ferrari, G., Galloway, A. C., Mignatti, P., and Pintucci, G. (2007) *J. Cell. Biochem.* **100,** 1100–1108
17. Bugler, B., Amalric, F., and Prats, H. (1991) *Mol. Cell. Biol.* **11,** 573–577
18. Couderc, B., Prats, H., Bayard, F., and Amalric, F. (1991) *Cell Regul.* **2,** 709–718
19. Quarto, N., Finger, F. P., and Rifkin, D. B. (1991) *J. Cell. Physiol.* **147,** 311–318
20. Bikfalvi, A., Klein, S., Pintucci, G., Quarto, N., Mignatti, P., and Rifkin, D. B. (1995) *J. Cell Biol.* **129,** 233–243
21. Coffin, J. D., Florkiewicz, R. Z., Neumann, J., Mort-Hopkins, T., Dorn, G. W., II, Lightfoot, P., German, R., Howles, P. N., Kier, A., and O'Toole, B. A. (1995) *Mol. Biol. Cell* **6,** 1861–1873
22. Vagner, S., Touriol, C., Galy, B., Audigier, S., Gensac, M. C., Amalric, F., Bayard, F., Prats, H., and Prats, A. C. (1996) *J. Cell Biol.* **135,** 1391–1402
23. Bikfalvi, A., Klein, S., Pintucci, G., and Rifkin, D. B. (1997) *Endocr. Rev.* **18,** 26–45
24. Hogrefe, H. H., Hogrefe, R. I., Walder, R. Y., and Walder, J. A. (1990) *J. Biol. Chem.* **265,** 5561–5566
25. Cummins, L. L., Owens, S. R., Risen, L. M., Lesnik, E. A., Freier, S. M., McGee, D., Guinosso, C. J., and Cook, P. D. (1995) *Nucleic Acids Res.* **23,** 2019–2024
26. Stein, D., Foster, E., Huang, S. B., Weller, D., and Summerton, J. (1997) *Antisense Nucleic Acid Drug Dev.* **7,** 151–157
27. Shine, J., and Dalgarno, L. (1974) *Proc. Natl. Acad. Sci. U. S. A.* **71,** 1342–1346
28. Hui, A., and De Boer, H. A. (1987) *Proc. Natl. Acad. Sci. U. S. A.* **84,** 4762–4766
29. Matveeva, O. V., and Shabalina, S. A. (1993) *Nucleic Acids Res.* **21,** 1007–1011
30. Mignone, F., and Pesole, G. (2002) *Appl. Bioinformatics* **1,** 145–154